ANNUAL REVIEWS

Storage of Carbon Dioxide in Saline Aquifers: Physicochemical Processes, Key Constraints, and Scale-Up Potential

Philip S. Ringrose,[1,2] Anne-Kari Furre,[1]
Stuart M.V. Gilfillan,[3] Samuel Krevor,[4] Martin Landrø,[5]
Rory Leslie,[3] Tip Meckel,[6] Bamshad Nazarian,[1]
and Adeel Zahid[1]

[1]Equinor Research Center, 7053 Trondheim, Norway; email: phiri@equinor.com

[2]Department of Geoscience and Petroleum, Norwegian University of Science and Technology, 7012 Trondheim, Norway

[3]School of GeoSciences, University of Edinburgh, Grant Institute, EH9 3FE Edinburgh, Scotland

[4]Department of Earth Science & Engineering, Imperial College, SW7 2BU London, United Kingdom

[5]Department of Electronic Systems, Norwegian University of Science and Technology, 7012 Trondheim, Norway

[6]Jackson School of Geosciences, The University of Texas at Austin, Austin, Texas 78705, USA

ANNUAL REVIEWS CONNECT

www.annualreviews.org

- Download figures
- Navigate cited references
- Keyword search
- Explore related articles
- Share via email or social media

Keywords

CO$_2$ storage, CO$_2$ capture and storage, CCS, geophysics, geochemistry, monitoring, dissolution

Abstract

CO$_2$ storage in saline aquifers offers a realistic means of achieving globally significant reductions in greenhouse gas emissions at the scale of billions of tonnes per year. We review insights into the processes involved using well-documented industrial-scale projects, supported by a range of laboratory analyses, field studies, and flow simulations. The main topics we address are (*a*) the significant physicochemical processes, (*b*) the factors limiting CO$_2$ storage capacity, and (*c*) the requirements for global scale-up.

Although CO_2 capture and storage (CCS) technology can be considered mature and proven, it requires significant and rapid scale-up to meet the objectives of the Paris Climate Agreement. The projected growth in the number of CO_2 injection wells required is significantly lower than the historic petroleum industry drill rates, indicating that decarbonization via CCS is a highly credible and affordable ambition for modern human society. Several technology developments are needed to reduce deployment costs and to stimulate widespread adoption of this technology, and these should focus on demonstration of long-term retention and safety of CO_2 storage and development of smart ways of handling injection wells and pressure, cost-effective monitoring solutions, and deployment of CCS hubs with associated infrastructure.

INTRODUCTION

Reduction in global greenhouse gas emissions is a key issue for modern human civilization. An essential part of any cost-effective solution to this challenge is long-term storage of CO_2 in deep geological rock formations, a process referred to as geological CO_2 storage (GCS), CO_2 capture and storage (CCS), or carbon dioxide sequestration. (The terms carbon sequestration and carbon storage are often used erroneously as shorthand for geological storage of CO_2 molecules.) In this review, we consider only the case of geological storage of CO_2 captured from man-made sources and stored in saline aquifers, as we consider this to be the dominant vehicle for realizing globally significant levels of CCS (1). Other potentially significant forms of GCS include

- CO_2 storage as a part of CO_2-enhanced oil recovery (CO_2-EOR) (2, 3) or enhanced gas recovery (4, 5) projects. In these projects, CO_2 is injected into a partially depleted hydrocarbon field to recover a greater portion of the trapped oil or gas that remains in the reservoir rock pore space by both increasing the reservoir pressure and reducing the viscosity of the oil. Such projects are typically the main route for CO_2 capture, utilization, and storage concepts, where CO_2 use acts as an economic incentive owing to the revenue generated from production of additional hydrocarbons. Because the produced hydrocarbons lead to further CO_2 emissions when combusted, CO_2-EOR projects have net-positive CO_2 emissions to atmosphere but can be viewed as a route toward future negative-emission CCS projects.
- CO_2 storage in depleted gas and oil fields (6, 7).
- CO_2 storage in coal formations (8) either via injection of CO_2 into unmineable coal seams or as part of enhanced coal-bed methane projects (analogous to CO_2-EOR).
- CO_2 storage in igneous rocks [especially basalts (9)], where enhanced rates of mineralization of injected CO_2 can occur.

The reason we focus on storage in saline aquifers is partly to limit the review but also because important insights into the processes involved in CCS have been gained via well-documented industrial-scale saline aquifer storage projects (10–12). We also argue that CO_2 storage in saline aquifers offers the main solution to achieving globally significant reductions in greenhouse gas emissions (13), while accepting that GCS in oil and gas fields and in basaltic rocks may play a significant role in some geographies.

It is also worth stressing that CCS is not considered as an alternative to other key solutions to achieving reductions in greenhouse gas emissions, including greatly expanded use of renewable sources of energy, societal and lifestyle changes, changes in land use, and more efficient use of energy overall. In most projections, CCS is anticipated to support 10–15% of total cumulative emissions reductions through to 2050 (14). However, CCS is widely recognized as an essential part of the decarbonization process for modern human society, as it enables removal of CO_2 emissions

from existing industrial and energy systems, as well as supporting negative-emissions solutions (15). Indeed, the Intergovernmental Panel on Climate Change reviews of global warming, climate change impacts, and mitigation activities (16, 17) have repeatedly shown that global warming cannot be realistically mitigated without CCS. It should also be stressed that engineered geological storage of CO_2 is a well-established technology with more than 50 years of operational experience in CO_2 capture, utilization, and storage and 25 years of saline aquifer storage operations. Most notably, industrial-scale CCS using a saline aquifer started in 1996 with the Sleipner project in Norway (18).

We wish to address the following main questions:

1. What are the dominant physicochemical processes that occur during saline aquifer storage?
2. What have we learned about the constraints on CO_2 storage capacity?
3. How can this experience be applied toward strategy for global scale-up of CCS to meet climate mitigation targets?

We address these questions using various field cases but most frequently use the Sleipner case study as an illustration. This is arguably the best-documented and most-studied field case and certainly the longest-running saline aquifer storage project.

PHYSICOCHEMICAL PROCESSES

After CO_2 is captured at the surface from a CO_2 capture plant, the CO_2 must be transported to a wellhead for geological storage. The CO_2 must then be compressed to be injected at a sufficient pressure to enter the geological formation at the in situ pressure and temperature. This involves taking the CO_2 across the phase transition to be stored in the liquid or dense phase. **Figure 1** illustrates this phase transition for typical subsurface conditions in the North Sea. Fundamentally,
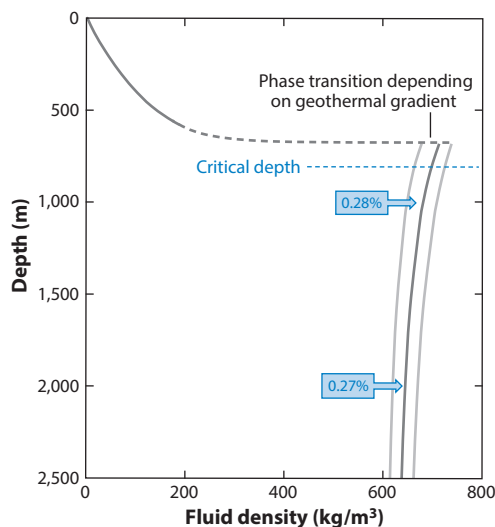

Figure 1

CO_2 density versus depth diagram for typical subsurface conditions in the North Sea. The black line is the density function at the Sleipner location assuming a geothermal gradient of 35°C/km (±2°C/km; *gray lines*) and a hydrostatic pore pressure gradient. The CO_2 phase transition occurs at somewhere between 550-m and 750-m depth, depending on local temperature, supporting the generally assumed critical depth of 800 m. Blue boxes show the relative volume occupied by CO_2 in the subsurface compared with surface volumes.

CO_2 is stored relatively deep (greater than $\sim$800 m) to ensure that CO_2 remains in a dense form—in either a liquid or supercritical phase. Regional differences in the geothermal gradient mean the critical depth for this phase transition varies. At intended storage depths, CO_2 has a density of approximately 700 kg/m^3 (slightly less dense than water) but at the same time has a viscosity more similar to that of hydrocarbon gases (CO_2 viscosity is $\sim$0.06 cP at 1,500 m depth). Therefore, an appreciation of CO_2 storage involves a substance that is unlike the water or hydrocarbon resources that have traditionally been the focus of subsurface reservoir engineering. Put simply, CO_2 in the subsurface has a liquid-like density and a gas-like viscosity. We have decades of experience in understanding, modeling, and monitoring CO_2 storage projects from both natural CO_2 stores and the growing collection of engineered storage sites. CO_2 has also been injected into reservoirs in many CO_2 EOR projects, and reservoir modeling of CO_2–brine–hydrocarbon systems is a relatively mature technology (19). Natural reservoirs of CO_2 derived from volcanogenic sources (20), notably several large accumulations in the Colorado Plateau and Rocky Mountains of the United States, can also be used to better appreciate the long-term processes acting on CO_2 retained in the subsurface over millions of years. Specifically, these natural analogs have been used to constrain CO_2 dissolution rates in the brine phase (21, 22) and the rates of long-term CO_2 migration and leakage along faults (23).

We can group the physicochemical processes that control the fate of CO_2 in a saline aquifer in terms of

1. the fluid dynamics of free-phase CO_2 in a brine-saturated porous medium;
2. the dissolution of CO_2 into the aqueous (brine) phase; and
3. the formation of minerals by chemical reaction with the CO_2 introduced into the saline aquifer.

These topics are more fully covered in several useful reviews and textbooks (1, 24–26), and here we identify recent insights and provide an update on the current state of knowledge. Note that the term free-phase refers to CO_2 that is not geochemically mixed with brine or minerals and is therefore potentially mobile as a separate fluid phase within the porous medium.

Fluid Dynamics of Free-Phase CO_2 in a Brine-Saturated Porous Medium

Injection of CO_2 into a brine-filled permeable rock formation is part of a class of multiphase flow problems that have been studied extensively (e.g., 1, 24). A two-phase CO_2–brine system is immiscible—the fluids are separated by a capillary interface. An important first approximation to the behavior of CO_2–brine systems is found via application of a set of dimensionless ratios that characterize the flow dynamics of two-phase immiscible flow systems (1, 27, 28). There are many ways of expressing these ratios, depending on the boundary conditions assumed; however, the most important ratios for CO_2 storage are the viscous/capillary ratio (N_{VC}) and the gravity/viscous ratio (N_{GV}), which for a 2D system [using the assumptions of (29)] can be expressed as

$$N_{VC} = \frac{u_x\,(\Delta z^2)\,\mu_{nw}}{k_{av}\,\Delta x\,(dP_c/dS_w)} \qquad\qquad 1.$$

and

$$N_{GV} = \frac{\Delta\rho\,g\,\Delta x\,k_{av}}{u_x\,\Delta z\,\mu_{nw}}, \qquad\qquad 2.$$

where u_x is the total flow velocity in the horizontal (x) direction, Δx and Δz are the system dimensions, μ_{nw} is the viscosity of the nonwetting phase (CO_2), k_{av} is the average permeability, $\Delta\rho$

is fluid density difference, g is the acceleration owing to gravity, and (dP_c/dS_w) is the capillary pressure gradient as a function of wetting-phase saturation.

Because the viscous force scales with flow velocity (a function of the applied pressure gradient), viscous forces will dominate close to the injection well (a few hundred meters) but then decay outward into the aquifer, where gravity and capillary forces will become increasingly important. The gravity force is controlled mainly by the fluid density difference but is also influenced by the vertical permeability and system anisotropy. Owing to the high dependence of CO_2 density on temperature, the in situ density may be difficult to determine accurately for some settings. For example, the CO_2 density at the Sleipner storage site varies from approximately 700 kg/m^3 near the injection well down to approximately 350 kg/m^3 at the top of the storage formation. Therefore, N_{GV} is variable, both spatially and over time. However, what is clear is that the interplay of viscous, gravity, and capillary forces results in an inverted cone shape for the CO_2 plume as it spreads into the aquifer and beneath a sealing caprock. A caprock is an informal term for a geological sealing system, typically comprising several mud-rock units that provide primary and secondary seals to the porous aquifer unit. This process is well understood in terms of guiding principles but is difficult to predict in detail in the real world (1, 24, 25). These concepts are usefully summarized in **Figure 2** (based on Reference 30), which also identifies the near-wellbore region where dry-out effects can occur (discussed in the next section).

The rate and degree to which capillary and gravity forces become important away from the injection well are difficult to determine for two main reasons: (*a*) Determining the changing value of the viscous/capillary ratio can be quite challenging, and (*b*) rock heterogeneity has a critical role that is difficult to predict and model. For a homogeneous porous media, capillary forces operate only at very small scales (at the pore scale and up to ~0.2 m) and have little impact at larger scales. However, heterogeneous reservoir rock formations (especially the effects of lamination and bedding) mean that effects of capillary forces can be quite significant at larger scales (27, 31, 32). One important effect is referred to as heterogeneity trapping, whereby small-scale heterogeneities (e.g., low-permeability layering at the scale of 0.01–0.1 m) cause retention of the nonwetting phase owing to capillary forces (**Figure 3**). These effects have been documented in many laboratory studies (33, 34), and models of CO_2 storage systems that account for heterogeneity trapping demonstrate that a significant amount of CO_2 storage is likely to be in the form of residual CO_2 saturation (35, 36).
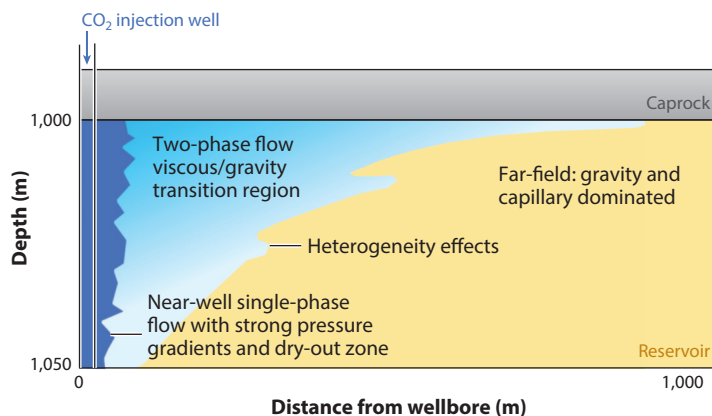

Figure 2

Sketch of flow processes and flow regimes for CO_2 injection into an idealized storage unit (figure modified from Reference 30).
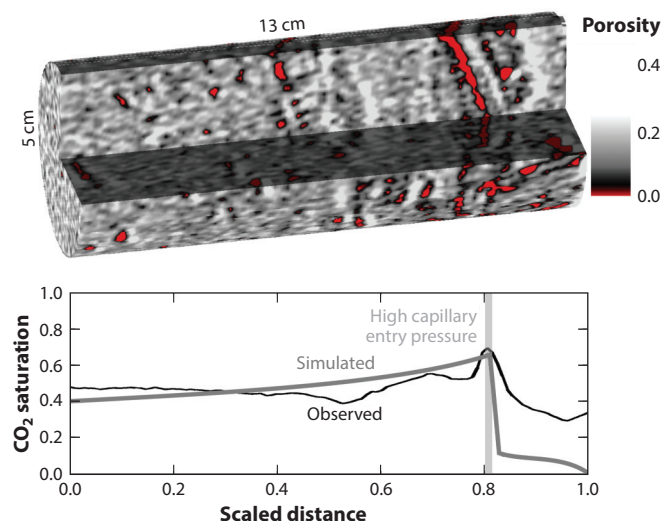
Figure 3

Trapping of CO_2 at high saturations upstream of a zone of high capillary entry pressure in an otherwise permeable sandstone rock. Heterogeneities in the form of low-permeability layers lead to more trapping than would be anticipated by the pore-scale capillary trapping mechanism alone and can contribute significantly to enhanced trapping of CO_2 in an aquifer (figure modified from Reference 31).

Another effect is that small-scale heterogeneities in the capillary pressure characteristics can significantly enhance or slow down the advancement of the plume (31, 37). CO_2 migration upward across pervasive sandstone bedding layers will be inhibited and sometimes trapped, as described above. When the CO_2 migrates laterally as a gravity current beneath a caprock, semi-parallel to layering, it will channel, sometimes in layers as small as centimeters in thickness, and the lateral migration rate will be enhanced significantly (as illustrated in **Figure 4**). Similarly, plume migration through isotropic heterogeneities of the type found in carbonate reservoirs, or through
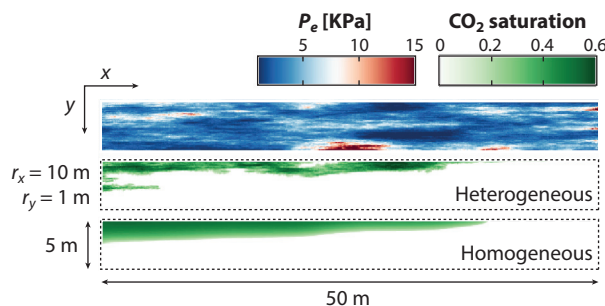

Figure 4

Simulations of CO_2 injected into reservoirs that are heterogeneous and homogeneous, respectively, in their capillary pressure characteristics, but otherwise share the same average properties. The heterogeneous distribution of capillary pressure, P_e, is shown in the top image, where r_x and r_y refer to the horizontal and vertical correlation lengths of the model. Layered heterogeneity in the capillary pressure (*middle image*) results in CO_2 channeling and more rapid lateral migration of CO_2 (figure modified from Reference 32).

networks of less-pervasive bedding planes, will channel in a way analogous to a river finding a path of least resistance for fluid flow, leading to enhanced plume migration.

Dissolution of CO_2 into the Aqueous Phase

The most important geochemical reaction for CO_2 storage in saline aquifers is dissolution of CO_2 into the brine phase. This process has an important role in stabilizing and securing long-term storage, but estimates of the effect vary enormously. We know that the process of molecular diffusion of CO_2 within a saline aqueous phase is very slow (24), and we also know that the convective mixing at the CO_2–brine interface is a much faster process, which is expected to dominate the rate of CO_2 dissolution. However, to initiate convective mixing, a diffusive boundary layer must develop and achieve a critical thickness before convection can occur. Using numerical analysis based on experimental data, Riaz et al. (38) estimated that the critical time (t_c) for onset of convection and the characteristic wavelength (λ_c) of the convection cells are in the range of 10 days $< t_c <$ 2,000 years and 0.3 m $< \lambda_c <$ 200 m. As with fluid flow and trapping, reservoir heterogeneity further complicates the dissolution problem. The presence of heterogeneity in the permeability field can either inhibit or enhance the dissolution rates, depending on the sedimentary architecture (39). In contrast, free-phase CO_2 channeling through small capillary heterogeneities dramatically increases the overall CO_2–brine interfacial area. This, in turn, significantly enhances mass transfer into the aqueous phase, such that CO_2 dissolution rates can even approach the same order of magnitude as the injection rate itself (40). Thus, reduction in this large range in a priori estimates requires more detailed knowledge of the geological architecture and permeability.

For the Sleipner case, for which we have relatively good knowledge of the aquifer properties, as well as good monitoring data to constrain the growth and geometry of the plume, we can estimate that the actual CO_2 dissolution rate is between 0.5% and 1% per annum, or between 10% and 15% of the cumulative injected mass after 20 years (41, 42).

Figure 5 shows example results from reservoir simulations of the Sleipner storage unit, with estimated ranges in the dissolved fraction. Here, the high-resolution 2019 Sleipner reference model grid (2 million cells, with vertical cell thickness of 2 m) was used with the E300 reservoir simulator package, where CO_2–brine mutual solubilities are calculated assuming fugacity equilibration between brine and CO_2 phase using the method and data from Reference 43. The simulation results show that by the time of the 2013 time-lapse seismic survey, the dissolved fraction was between 10.6% and 12.6% of the total CO_2 mass injected (**Figure 5a**). This estimate is consistent with laboratory data (44) and within the upper bound of the dissolved mass fraction that can be estimated by inversion of gravity field survey data (41). For longer-term forecasting (**Figure 5b**), the predicted dissolved fraction is very dependent on the vertical permeability assumption. For a low vertical-to-horizontal permeability ratio (k_v/k_h) (red curve in **Figure 5b**), CO_2 tends to migrate much faster laterally during injection, thereby increasing the dissolution of CO_2 by increasing the contact area of the CO_2–brine interface. For a higher k_v/k_h ratio (green curve in **Figure 5b**), initial dissolution is lower because the plume remains more compact and has a lower CO_2–brine interface contact area. However, after injection is stopped, the more compact plume (high k_v/k_h) continues to spread and promote further long-term dissolution. Convection-driven dissolution is not included in these simulations. Forecasting long-term dissolution rates therefore remains a significant challenge, although shorter-term rates can be constrained from site data and are expected to be approximately 10% of the total mass for the Sleipner case.

We can, however, use natural analogs to estimate the longer-term rates. Combined noble gas and stable carbon isotope analyses of gas samples from nine actively producing natural CO_2 reservoirs in the United States, Europe, and China indicate that dissolution of CO_2 is the dominant
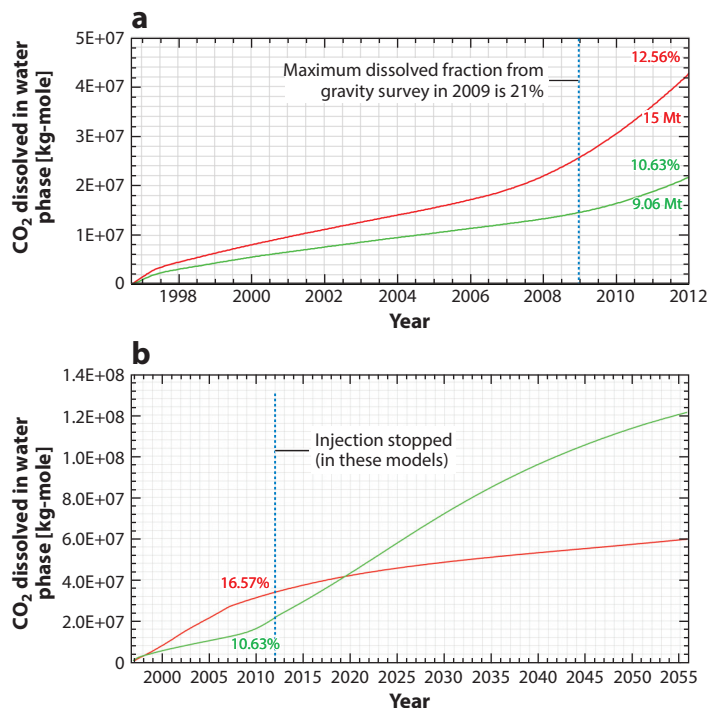
Figure 5

Example reservoir simulation models of the Sleipner storage site with estimated ranges in forecasts for the dissolved fraction. (*a*) Simulated dissolved fraction for the historical period: The green curve is the reference case with 0.6-Mtpa injection, and the red curve is for a 1-Mtpa rate; figures to the right give estimates at 2012; the maximum possible dissolved fraction is estimated from gravity survey data (41). (*b*) Long-term forecasts: The green curve is the reference case, with k_v/k_b ratio = 0.1, and the red curve is a corresponding low-vertical-permeability case with k_v/k_b = 0.0001. For both cases, 9.06 Mt CO_2 was injected up to 2012, when injection was stopped and the plume was allowed to stabilize with continuing dissolution. Simulations were done using the E300 simulation package (CO2Store option, with assumption based on Reference 43) and using the grid from the Sleipner 2019 benchmark model (co2datashare.org). Actual injection at the site is variable, between 0.6 Mtpa and 1 Mtpa, and continues to the present day.

storage mechanism over geological time in both siliciclastic and carbonate reservoirs (45–47). These studies showed that up to 90% of initially emplaced CO_2 in contact with sampled wells had been lost to dissolution. Furthermore, this work highlights that mineral precipitation is a minor sink, even after millions of years of CO_2 storage. More recent work using these methods identified that some 7 kt (thousand tonnes) of the ~1.5 Mt (million tonnes) of CO_2 injected into the Cranfield EOR field in Mississippi, USA (approximately 0.2%), had dissolved into the groundwater over an 18-month injection period (48). A significant additional proportion of CO_2 had also dissolved into the oil phase within the reservoir, enhancing recovery from the field.

Two recent studies (21, 49) have further demonstrated this approach, estimating both the total mass of CO_2 dissolution and the dissolution rate within the Bravo Dome CO_2 reservoir (New Mexico, USA). Sathaye et al. (21) used thermochronology to estimate the timing of CO_2 charge into Bravo Dome to be 1.2 to 1.5 million years. Using a specially constructed reservoir model, they determined that the mass of CO_2 currently retained within the reservoir is ~1.3 Gt (gigatonnes). Integrating this reservoir model with the previous geochemical measurements allowed

estimation of the total amount of CO_2 emplaced as ~1.6 Gt, where an estimated 366 ± 120 Mt ($22 \pm 7\%$) of this had dissolved. It is estimated that >40% of the CO_2 dissolution occurred during emplacement, with the remainder subsequently dissolving into the underlying aquifer. In one sector of the reservoir, the rate of CO_2 dissolution determined was 0.1 g/(m^{2}y), which exceeds the amount expected from CO_2 diffusion alone, implying that convective mixing of CO_2 and water had occurred.

In contrast, Zwahlen et al. (49) took an alternative approach, modeling noble gas and stable isotope diffusion profiles from the gas–water contact through the gas column to obtain a much younger estimate of CO_2 emplacement within Bravo Dome of 14,000–17,000 years ago. This work also calculated the amount of CO_2 lost to dissolution within the field, producing a larger estimate of 506 ± 166 Mt, indicating a significantly higher dissolution rate of $48 +19/-17$ g/(m^{2}y) to 58 ± 20 g/(m^{2}y). Although to date CO_2 dissolution rates have been constrained from only a single natural analog, and vary considerably, the work highlights the potential of the geochemical methods involved in assessing the effectiveness of different CO_2 trapping mechanisms, particularly if tracers inherent within the captured CO_2 are used (50, 51). The work also emphasizes that a thorough understanding of the hydrogeological setting of prospective CO_2 stores is essential for accurate prediction of the long-term fate of the injected CO_2.

Mineralization of CO_2

Introducing CO_2 into a saline aquifer unit will modify the natural chemical balance and potentially cause dissolution or precipitation reactions. Carbon dioxide is a common component of the subsurface rock system (it is the most abundant subsurface fluid in the crust apart from water), occurring both as a dissolved component of aqueous fluids (groundwater) and as a free/mobile gas phase. The main sources of naturally occurring CO_2 are (*a*) from volcanic systems, with the CO_2 being sourced from the deep mantle (22), and (*b*) from gas generated from buried biogenic sources. The major natural accumulations of CO_2 in North America (e.g., Bravo Dome, New Mexico, and Sheep Mountain, Colorado), which are used as sources for CO_2 EOR projects, contain CO_2 predominantly originating from the mantle. CO_2 is also produced from a wide range of biologically sourced systems, including decomposition of organic matter, methanogenesis (a byproduct of methane-producing microbes), oil-field biodegradation, hydrocarbon oxidation, and decarbonation of marine carbonates.

When introducing CO_2 into a saline aquifer, the main question is how the additional CO_2 might modify or perturb existing chemical reaction processes. Will some of the CO_2 precipitate as minerals (usually carbonate minerals or clays minerals), or could some dissolution occur? Some general conclusions can be made based on geological data from natural analogs (52):

- When CO_2 is added to siliciclastic rocks, such as sandstones, as soon as the formation water is saturated with CO_2, the injected CO_2 will simply remain as a separate phase. Over centuries or longer, feldspar group minerals may react with CO_2 that has dissolved into the reservoir brine to form carbonates and clays (53).
- In the case of CO_2 injection into carbonates (or rocks with carbonate cements), some dissolution of carbonate minerals will occur, but again, as soon as the formation water becomes saturated with CO_2, the injected CO_2 will remain as a separate phase.

Experience from early CO_2 storage injection projects, such as Sleipner, In Salah, and Snøhvit, confirms that geochemical reactions are slow and relatively minor (54, 55), with virtually all the CO_2 remaining as a separate (liquid, gas, or dense) phase. In an analysis of data from a natural CO_2 reservoir (a CO_2-rich gas field), Wilkinson et al. (56) showed that 70–95% of the CO_2 is present

as a free phase, after tens of millions of years, with only approximately 2.4% of the CO_2 stored in the mineral phase and a similar amount dissolved in the pore waters. The finding here is that although dissolution and precipitation reactions do occur when new CO_2 is introduced into the subsurface, the CO_2 quickly establishes a new chemical equilibrium with the in situ pore waters, following which reaction rates are very slow. CO_2 dissolution into the brine phase can, however, be significant (see above).

When CO_2 is put into contact with clay minerals, possible reactions and effects become rather complex. For example, in the case of CO_2 storage in shales (57), gas sorption can lead to significant CO_2 storage capacity in shale sequences. Geochemical reactions, such as dissolution of silicate minerals and precipitation of carbonate minerals, may also have a measurable effect on the porosity, permeability, and diffusion properties of shales.

For the case of sandstone saline aquifers (siliciclastic sedimentary systems), although some trapping of injected CO_2 as a mineral phase can occur, the reaction rates are very slow. Some dissolution of carbonate minerals may also occur, but again at very slow rates. An analysis of potential geochemical reactions at the Sleipner CO_2 injection site over a period of 10,000 years into the future (58) showed that geochemical reactivity of the Utsira sandstone is rather low, with mineral trapping making only minor contributions to CO_2 storage.

Another focus of geochemical-reaction analysis for storage has focused on the near-wellbore environment, where carbonate minerals may be formed when calcium hydroxide (Portlandite cement) reacts with CO_2. In a detailed study of geochemical modeling and experiments of brine–CO_2 reactions with wellbore cement, Carroll et al. (59) found that although important reactions can occur (precipitation of amorphous silica, calcite, and aragonite), the reaction of the hydrated cement with synthetic brine occurs rapidly (usually within 5–10 days). Geochemical modeling (60) to assess the potential impacts of the observed reactions indicated that these mineral products act to retard the rate of CO_2 migration, which might occur along potential interfaces (e.g., cement–rock interface), implying that mineralization will tend to seal up potential leakage points in the near-wellbore environment.

In contrast, CO_2 storage in basalts (and other basic igneous rocks) results in very high rates of mineralization, as demonstrated at the CarbFix injection site in Iceland, where approximately 80% of CO_2 injected at a depth of 500–800 m within hot basaltic rocks was found to be carbonated as minerals within one year (9, 61). Although CO_2 storage in basalts is very different from saline aquifer storage, the insights may be relevant, especially where saline aquifer sandstone formations are interbedded with volcanic rocks, where enhanced mineralization of CO_2 can occur, as has been the case in Australian natural CO_2 reservoirs in the Otway Basin (62).

CONSTRAINTS TO REALIZING CO_2 STORAGE CAPACITY

Injectivity and Well Constraints

There are two fundamental constraints on CO_2 storage in a saline aquifer: the ability of the well(s) to inject CO_2 at the require rates and the ability of the aquifer formation to take the total CO_2 volumes. Geological limits on capacity are reviewed below, whereas the well constraints are reviewed here. The two are, however, closely interrelated. For a CO_2 injection well, there are two main pressure gradients to consider: (*a*) from the wellhead pressure, P_{wh}, to the bottom-hole pressure, P_{bh}, and (*b*) from the bottom-hole pressure, P_{bh}, into the saline reservoir formation, P_{res}. The first involves an increasing pressure gradient and the second a decreasing gradient, with P_{bh} normally being the maximum pressure in the system. Thermal effects can lead to significant pressure variations, meaning that pressure estimation away from measurement points may be challenging but tractable using an equation of state (EOS) and reservoir simulation software. The Peng–Robinson

and Soave–Redlich–Kwong equations are two commonly used EOS, which, because they are relatively simple to implement (cubic equations), are widely used in modeling packages (63). The Span–Wagner EOS provides more accuracy for understanding detailed system behavior and complex mixtures (64) but is more demanding for numerical simulation.

Experience from operating wells shows that the flowing bottom-hole pressure may take several hours to stabilize toward the shut-in bottom-hole pressure owing to thermal equilibration. Pressure gradients in the wellbore system can, to some extent, be controlled via appropriate choice of tubing diameter and use of wellhead or downhole chokes. For injection into formations with depleted reservoir pressure, heating of the CO_2 stream may be required to avoid transition into the vapor phase, as was undertaken at the K12-B test site in the Netherlands (65).

Assuming that the P_{bh} can be controlled by the design of the well and surface compression facilities, the flow rate from the well into the formation can be estimated using the radial Darcy flow equation, which, assuming a vertical well geometry, has the form (26)

$$q = \frac{2\pi k_{res}\, h_i\, (P_{res} - P_{bb})}{\mu\, \ln(r_e/r_w)}, \qquad 3.$$

where q is the CO_2 flow rate, k_{res} is the permeability of the rock formation, h_i is the height of the injection well interval (the completion interval), μ is the fluid viscosity, r_e is the effective radius of the reservoir unit, and r_w is the radius of the well itself. The far-field formation pressure, P_{res}, is usually assumed to be constant but could gradually increase for the case of injection into a confined aquifer (e.g., a small fault block) or could decrease over time in the case of hydrocarbon production from gas fields in hydraulic communication with the injection unit (66). **Figure 6** summarizes the likely pressure gradients in the vicinity of an injection well, showing a possible wellbore damage effect. The Injectivity Index (II) (a ratio of flow rate to pressure gradient) may
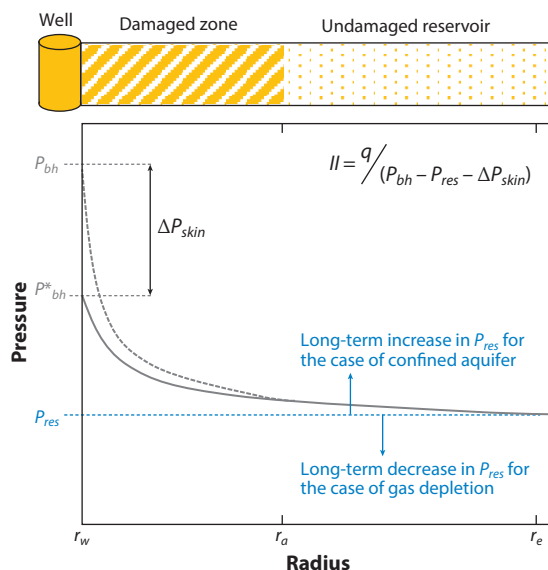

Figure 6

Pressure gradients around an injection well, with possible effects of near-wellbore damage or pore clogging, and possible longer-term trends in the far-field pressure. A simple form of equation for the Injectivity Index (II) is shown, where ΔP_{skin} refers to the additional pressure gradient owing to near-wellbore effects.

be strongly influenced by these wellbore damage effects, causing the P_{bh} to be much higher than the expected pressure (P^*_{bh}) without wellbore damage effects.

Experience from several projects (e.g., Sleipner, Snøhvit, and Quest) reveals unexpected variability in the injectivity performance in the early phases of projects (26, 67). Reasons for reduced injectivity performance include formation collapse near the well (Sleipner), formation of salt precipitates owing to reaction of CO_2 with brines (Snøhvit and Quest), and the migration of fine particles that plug the rock pores (possibly at Snøhvit). To illustrate the typical magnitude of these near-wellbore effects, in the case of Sleipner, the first months of injection witnessed a tenfold reduction in injectivity owing to near-wellbore formation collapse and corresponded to a rise in P_{bh} of approximately 20 bars (26). In the case of Snøhvit, the first months of injection showed a fluctuating reduction in injectivity caused by salt precipitation and pore clogging and corresponding with a rise in P_{bh} of approximately 50 bars (68). In both cases, well interventions were applied to resolve the problems, and subsequent injection returned to close to the expected levels. At Sleipner, a new completion interval with gravel and sand screens was applied (67, 69), and at Snøhvit, a methyl–ethylene–glycol solution was added to the injection stream (68). Injectivity constraints are therefore potentially significant but are likely to be resolved as part of the early-phase well management and optimization process. However, in several cases, the encountered formation permeability in a CO_2 appraisal well was significantly lower than expected and insufficient for injection to proceed (70). In such cases, hydraulic fracturing could be used to enhance injectivity (70), or the well may need to be abandoned in search of alternative injection horizons/locations.

Trap Capacity and Pressure Limits

The capacity of the intended geological storage units is one of the most critical and debated aspects of saline aquifer storage. Different types of capacity estimates can be summarized by the techno-economic resource–reserve pyramid, in which several stacked capacity terms can be differentiated (71):

- a theoretical capacity (the physical limit);
- an effective capacity (an estimate using cut-off criteria);
- a practical capacity (considering economic, technical, and regulatory factors); and
- a matched capacity (site-specific storage realized for specific CO_2 projects).

Typically, national storage resource mapping projects use a form of effective capacity (e.g., 72–74), whereas industrial and engineering associations are more focused on practical and matched capacity estimates as a basis for investment decisions (75). The capacity of the Utsira formation offshore Norway (an extensive shallow marine sandstone of Miocene age), which hosts the Sleipner CO_2 storage project, has been much studied in terms of future storage potential. CO_2 storage capacity estimates for the Utsira Fm range between 1 and 60 Gt depending on assumptions made (76), ranging from the exploitation of structural traps only (at the low end) to development concepts using multiple wells, residual trapping, and pressure management (at the high end). However, the investable resource (i.e., a matched capacity) in terms of currently known and accessible prospects within the Utsira is estimated at approximately 0.17 Gt (76), which illustrates the challenge in going from a potential storage resource to an investible resource for project planning.

The underlying physical process that controls CO_2 storage efficiency in saline aquifers is that injection of a low-viscosity, buoyant, nonwetting phase into a water-saturated porous medium is fundamentally inefficient. The ratio of the actual volume of CO_2 stored to the theoretical pore volume available is termed the storage efficiency, ε (77), and represents the cumulative effects of heterogeneity, fluid segregation, and sweep efficiency. Analytical analysis using multiphase flow

theory supported by empirical site data suggests that ε is in the range of 0.005 to 0.06 (i.e., less than 6% of the pore volume), with values of 0.04 or 0.05 being typical assumptions for regional storage resource mapping projects (72–74). The estimate for the well-documented Sleipner case is that ε had reached approximately 0.052 (26) by the time of the time-lapse seismic survey of 2013. There are also several potential ways to increase ε above 0.06, by using smart well placements to exploit the geology (78, 79) or by modifying the injection stream (80). Filling of a structural closure (i.e., a geological trap) could allow ε to exceed 0.5 within the closure, although there is no documented demonstration of this to date.

Similar to the process of exploitation of hydrocarbon resources, in which various injection and production strategies are used to enhance recovery, it is theoretically possible to increase the storage capacity of a given reservoir by applying some advanced injection techniques designed to control the movement of CO_2 in the saline aquifer. These strategies can collectively be called mobility control techniques and aim at stabilizing the CO_2 front in the reservoir. This can be achieved in various ways using techniques adopted from hydrocarbon production. Water-alternating-gas injection is a well-documented technique used in oil production to reduce unstable fingering of the injected gas stream and to increase sweep efficiency. A similar scheme can be used in CO_2 injection to achieve control over CO_2 plume movement by injecting slugs of modified CO_2 stream following cycles of pure CO_2 injection. The bulk properties of CO_2 can be modified in various ways by using chemical additives, such as polymers or nanoparticles, or by intentionally fluctuating the temperature (80).

There are several ways of enhancing the CO_2 storage capacity via brine production to relieve the pressure (81, 82), an approach that has been implemented at the Gorgon CCS project in Australia. The disposal of produced brine has environmental and financial implications (83) but if properly managed has the potential to enhance storage resources in future projects. For the case of CO_2 injection into a confined geological system (e.g., a fault block with low-permeability barriers), the storage efficiency may be much lower, e.g., $\varepsilon < 0.01$ (84). However, most geological systems have imperfect seals, allowing some pressure dissipation, so that closed system models are overly pessimistic. Basic rock and fluid compressibility arguments can be used to show that storage sites must be situated within fault blocks large enough to allow adequate pressure dissipation (e.g., a 5-Mt injection requires a gross rock volume of $>2,500$ km^3 for a sealed boundary case) (26). For real systems, 3D fault architecture at the basin scale likely leads to some points of pressure communication through zones with lower fault displacement or fault zones with sand-to-sand juxtapositions.

For such confined geological systems, the storage capacity depends very much on the pressure history. Depleted reservoirs (owing to previous hydrocarbon extraction) can allow for higher storage efficiencies owing to the lower average pressure when injection begins. The same is true for aquifers under continuous depletion. This can occur if the storage reservoir is in hydraulic communication with a producing hydrocarbon reservoir. While hydrocarbon extraction is taking place, the storage units can experience considerable depletion, depending on the rate of extraction and the degree of pressure communication. The Smeaheia saline aquifer system located in the east of the Troll field, offshore Norway, is an example of such a system (66). **Figure 7** shows a cross-section through a geological model of the Smeaheia storage prospects along with dynamic flow simulation results showing the distribution of the CO_2 plumes after injection of 2.4 Gt CO_2 from four (hypothetical) injection wells located at the southern parts of the aquifer and completed in both the shallower pressure-depleted Viking group aquifer and the deeper Dunlin Group aquifers that are expected to remain mainly undepleted. A low-saturation plume is spread over a larger area in the depleted reservoir, whereas higher-saturation and more localized plumes are simulated for the deeper formations at close to hydrostatic pressure (**Figure 7b**). Thus,
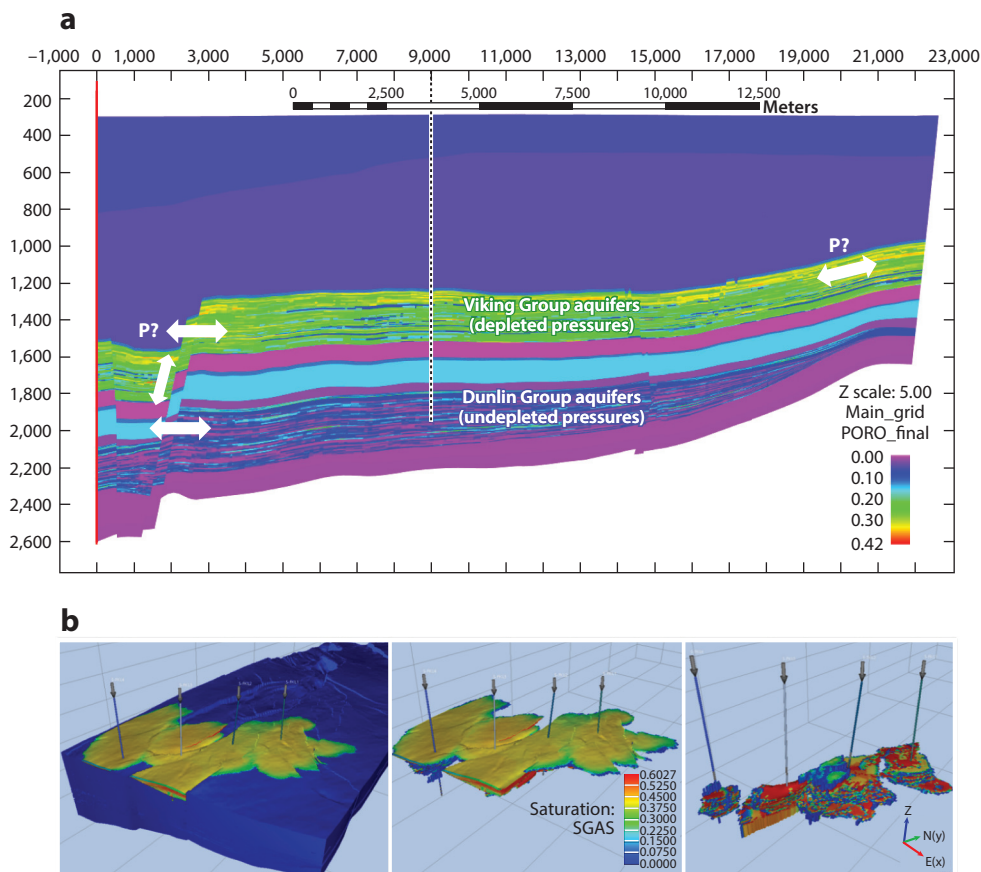
a

b

Figure 7

(*a*) Example cross-section through a geological model of the Smeaheia storage prospects (WNW-ESE section through the Gamma structural closure), with white arrows indicating the main pressure communication points described by Wu et al. (117) (section is 22 km wide and 2.5 km thick; color tone shows porosity). (*b*) Example flow simulation model in which 2.4 Gt of CO_2 has been injected in both the pressure-depleted Viking group aquifer and the undepleted Dunlin Group aquifers. The CO_2 plume is shown after 100 years of injection. (*Left*) Location of the four injectors at southern part of the aquifer. (*Middle*) CO_2 plume in the depleted Viking group. (*Right*) High saturation and localized plume in the deeper Dunlin Group. Simulations were done using the E300 reservoir simulator package.

although pressure limits may constrain storage capacity for certain cases, hydraulic connection to surrounding aquifers is likely to allow pressure dissipation. Effects of previous and concurrent pressure depletion will require dynamic flow simulation but can significantly improve or enhance long-term storage capacity (66).

Monitoring to Optimize and Confirm Successful Storage

Monitoring is important to establish a license to operate for CO_2 injection projects. The site operator must adhere to legal requirements to demonstrate that the CO_2 is safely contained in the subsurface. Legal frameworks typically include requirements that the monitoring should demonstrate that the CO_2 is migrating as predicted in the subsurface, that it is safely contained, and that there is no risk of negative impact on the environment. Establishing effective ways to monitor CO_2

storage projects has drawn a lot of attention over the last two decades, and there are now several best-practice documents, reviews, and textbooks on this topic to guide future projects (e.g., 85–87). Although many of the successfully applied methods were originally developed for petroleum reservoir monitoring, CO_2 storage monitoring additionally involves a unique set of challenges related to the physical properties of CO_2 in the subsurface and a wide set of concerns around ensuring safe long-term storage. There is widespread agreement that the most effective tool for monitoring subsurface CO_2 migration in the reservoir is the use of repeat seismic imaging (4D seismic), which has been used successfully at the Sleipner (88), Snøhvit (68), In Salah (89), Ketzin (90), Tomakomai (91), Quest (92), and Aquistore (93) saline aquifer storage projects. Other important monitoring technologies include time-lapse gravity surveys, time-lapse resistivity logging downhole, and use of natural and artificial geochemical tracers (94, 95).

A key objective in 4D seismic monitoring of CO_2 storage is the detection limit to establish the minimum threshold thickness for a CO_2 layer. Both the thickness and the velocity of a CO_2 layer typically change during injection, and it is challenging to discriminate between the two effects (or to estimate both simultaneously) from conventional stacked seismic data, particularly as long as the layers are below tuning thickness (96–98). **Figure 8** illustrates this challenge. As CO_2 is introduced into the aquifer unit, the velocity decreases significantly (**Figure 8*a***), setting up a strong amplitude contrast in the system. However, below the tuning thickness, it is not possible to discriminate between the top and base of the layer from seismic data; hence, the thickness is undetermined (**Figure 8*b***). The nonmonotonic behavior of the velocity as a function of CO_2 saturation further adds to this complexity, as it introduces an uncertainty in the time-thickness transformation. Above the tuning thickness, it is possible to separate the top and base of the layer and improve velocity constraints (98). This underlines the need for precise and highly repeated time-lapse seismic data but also the need for other methods if the aim is to constrain the thickness and saturation change determination. Despite these challenges, the seismic monitoring of Sleipner has led to important insights into how the CO_2 migrates in the subsurface, and the site has been used to test
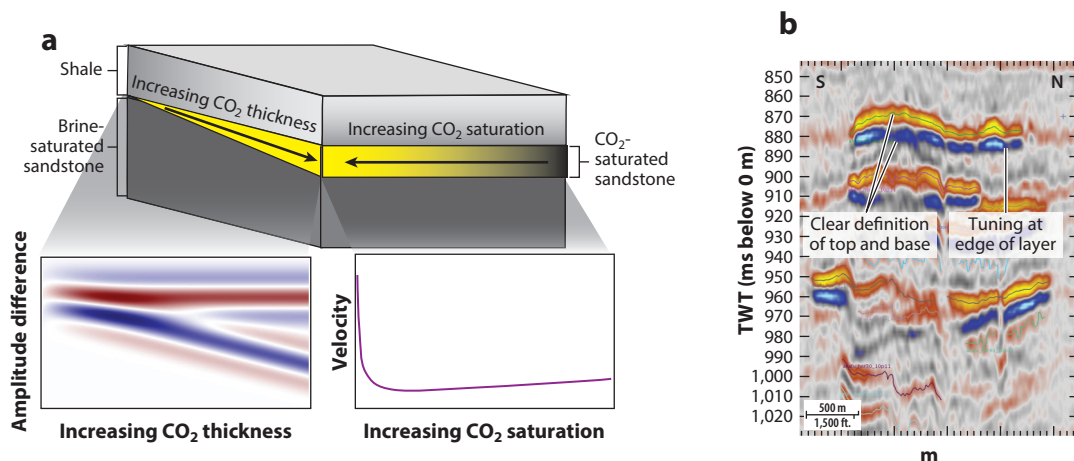
Figure 8

Illustration of the challenges in detecting thin layers with unknown CO_2 saturation from seismic data. (*a*) A wedge model of a CO_2 layer with varying thickness and saturation, showing that amplitude changes depend on both the saturation-dependent velocity and layer thickness, whereas velocity is strongly dependent on CO_2 saturation. The velocity model assumes homogeneous fluid distribution in the pore space. (*b*) Example cross-section through the 2010 seismic amplitude data at Sleipner showing amplitude variation for the CO_2 plume in Layer 9 (*top layer*).

dynamic flow models (99, 100). In particular, the degree to which CO_2 migration in the storage domain is controlled by the gravity-viscous ratio (Equation 2) or is dominated by capillary forces (Equation 1) has been significantly improved (101, 102) using the Sleipner seismic imaging data sets for calibration. Although this question is not fully resolved, the flow system is clearly gravity dominated, and understanding vertical migration paths and migration flow dynamics is the key remaining challenge (32).

In the case of thin horizontal CO_2 layers, the use of long-offset data or repeated refraction-type seismic data (103) is a useful complement to conventional 4D seismic data. When a seismic wave is propagating horizontally, the detectability increases because the wave spends more time in the thin CO_2-saturated layer. Typical examples of such waves are head-waves and diving waves. In full-waveform inversion, such waves play an important role in stabilizing the seismic inversion process (104, 105).

If the storage unit is less permeable and the injection pressure increases owing to low injectivity, there is a need to discriminate between fluid saturation and pore pressure changes (106). A case study from the Snøhvit field (107) shows that use of prestack time-lapse seismic data (or near and far offset stacks) is one way to resolve this issue. Another way to resolve this is to combine various geophysical methods, for instance, time-lapse seismic and time-lapse gravity (108). The development of accurate seabed gravimeters (109) is an important contribution to making this possible.

Fiber-optic-based monitoring systems are currently in rapid development and have already been successfully applied for storage monitoring, with demonstrations of downhole distributed acoustic sensing for time-lapse monitoring of CO_2 plumes at the Aquistore (66) and Quest (110) projects. Use of downhole and surface downhole distributed acoustic for 4D seismic monitoring has great potential for reducing monitoring costs, as has been demonstrated recently at the onshore injection projects Aquistore and Quest in Canada (93, 110).

Another important concept is the trigger survey philosophy, in which a basic routine monitoring strategy is established with additional survey options that are deployed only when an anomaly requiring further verification is detected. This is a key strategy in reducing monitoring costs. Furthermore, monitoring should ideally be considered as a beneficial activity ensuring an overall cost benefit for the lifetime operation of the storage project. In a study of ways to optimize offshore monitoring, the typical costs of monitoring based on historical experience at Sleipner and Snøhvit were estimated to be of order €2/t (for a 2015 reference) (111). Although this cost could potentially be reduced further, it is a small fraction of total project costs and will ideally pay for itself in terms of avoided costs of project stoppages or avoidable well operations.

STRATEGIES FOR GLOBAL SCALE-UP TO MEET CLIMATE MITIGATION TARGETS

Even though CCS is widely considered a proven technology—currently 19 large-scale CCS facilities are in operation, along with a further 4 under construction, which together have an installed capture capacity of 36 Mtpa (112)—a significant scale-up in CCS deployment is needed to meet the stated ambitions for emissions reduction in the next three decades. CCS is projected to provide 10–15% of total cumulative emissions reductions through 2050, requiring annual storage rates in 2050 in the range of 6,000–7,000 Mtpa (13). And even though the recent Intergovernmental Panel on Climate Change report on global warming (16) presents a range of illustrative model pathways with differing levels of assumed CCS, all the pathways require a significant CCS component. Cumulative storage growth rates in CCS deployment of at least 9% (113) are required, and with peak injection rates of up to 40–60 Gtpa by 2100. The total geological storage resource base required

is not expected to exceed 2,700 Gt of capacity in underground reservoirs and may be significantly less (113).

In developing a strategy to meet these CO_2 storage goals, it is useful to consider a continental-scale geological framework for future saline aquifer storage. An analysis of global offshore continental margins (13) demonstrates that ample storage resources are available, and that these resources are typically close to major industrial hubs and megacities, which are commonly located near major rivers feeding suitable offshore sedimentary basins. The major challenges for CCS scale-up are not geological but are about financial incentives and business drivers. Public perception factors also play an important role in both resisting or encouraging CCS as a climate mitigation measure. Some form of societal incentive for CCS is needed, with carbon taxes, tax rebates, emissions standards, and infrastructure investment funds usually dominating the sociopolitical discourse (114). The analysis of storage on offshore continental margins (13) suggests that approximately 12,000 CO_2 injection wells will be needed globally by 2050 to achieve the Paris Agreement goals. By using historic petroleum well rates as a proxy for potential future regional CCS well deployment, characteristic build-up rates can be estimated. **Figure 9** shows well build-up rates for an illustrative continental CCS cluster (based on the historic Norway well database). Approximately 5 such clusters would be needed to meet global CCS targets by 2050, with each cluster needing approximately 200 wells by 2030 and 1,000 wells by 2040. In practice, it is more likely that approximately 10–20 smaller CCS hubs will emerge, focused around major national industrial clusters. These projected CO_2 well rates are significantly lower than the historic petroleum industry drill rates, indicating that decarbonization via CCS is a highly credible and affordable ambition for modern human society. For reference, more than 1 million hydrocarbon wells were active in the United States in 2014 (the peak year to date) (115). The costs of saline aquifer storage (not reviewed here) depend very much on the injection depth, geological setting, and dimensions of the project, with reported cost estimates in the range of €2–20/tonne (2009 prices) (116). Onshore projects are generally cheaper than offshore projects, and large-scale CCS hubs will likely be the most effective means of reducing costs toward the lower end of this range.
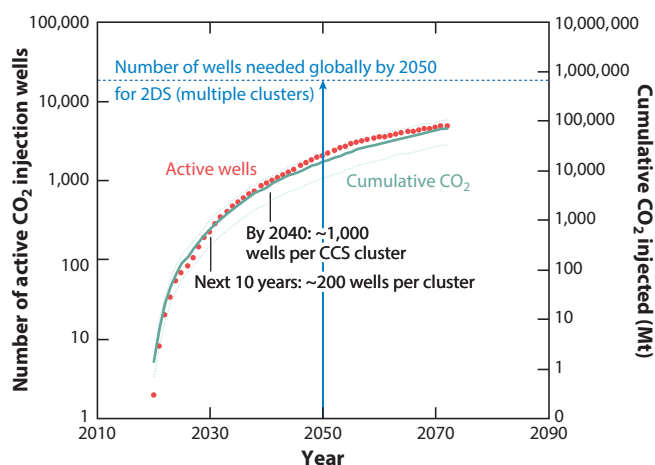
Figure 9

Characteristics of a continental CCS cluster with well build-out rates based on the historic Norway well database. Cumulative CO_2 estimate is based on empirical well data with mean (*bold lines*) and P10–P90 range (*dotted lines*) using methods explained in Reference 13. Abbreviations: 2DS, two-degree scenario; CCS, CO_2 capture and storage.

SUMMARY AND CONCLUSIONS

We have reviewed the current state of knowledge for CO_2 storage in saline aquifers, using available large-scale field observations supported by laboratory data. During the project lifetime (nominally approximately 25 years), the CO_2 is primarily trapped as a free phase within the brine-saturated porous medium, with an interplay of viscous, gravity, and capillary forces controlling fluid dynamics. Plume dynamics are macroscopically controlled by the viscous-gravity ratio, but capillary forces at the pore and bedding scale result in highly episodic migration behavior. Dissolution of CO_2 into the brine phase occurs slowly but steadily (as a function of temperature and salinity) and is found to be in the range of 10–13% after 17 years of injection for the Sleipner case. Study of natural CO_2 reservoirs, which are analogs of long-term geological storage, shows that hundreds of Mt of CO_2 can be trapped by dissolution over geological timescales. However, current estimates of the dissolution rate cover a wide range, from 0.1 to 58 g/(m^{2}y), and more complete constraint of this important parameter is an active area of research. The fractionation of CO_2 into mineral phases is extremely slow in most saline aquifer settings, such that mineral trapping makes only a minor contribution to CO_2 storage, even over periods of thousands of years. This strongly contrasts with the case of CO_2 storage in basalts, where storage of CO_2 as a mineral phase can dominate.

The main constraints on CO_2 storage in saline aquifers are related to injectivity limits and rock formation capacity. Injectivity challenges have been encountered in some projects but are generally solvable through use of established well-management and intervention technology. The total formation capacity for CO_2 storage is generally less than 6% of the available pore volume, owing to the inherent inefficiency of the fluid dynamics of a low-viscosity buoyant immiscible fluid entering a water-wet porous medium. Monitoring of injected CO_2 as it migrates as a plume away from the injection point using time-lapse seismic surveys has proven to be a highly effective method for guiding project operations and for demonstrating storage assurance (termed conformance and containment in permit regulations). Continuing advances in geophysical imaging, especially using low-cost fiber-optic sensing, mean that CO_2 storage monitoring programs are likely to increase in accuracy at reduced cost. Although concerns about possible CO_2 leakage are important to acknowledge and address, a wide set of geophysical and geochemical diagnostic tools are available to assess anomalies.

Pressure barriers and the size of the geological unit in hydraulic communication with the injection horizon can further reduce these capacity limits. Despite these physical limits to storage capacity, the numerous thick accumulations of porous sandstones in the world's sedimentary basins (especially offshore continental margins) provide more-than-sufficient storage capacity for the required CCS deployment in the coming decades. CCS deployment must grow from the current level of 36 Mtpa to more than 6,000 Mtpa by 2050, with a ceiling on rates of 40–60 Gtpa before 2100 to meet the emissions-reduction requirements implied by the two-degree warming scenario. This growth in CCS activity requires a CO_2 injection well-drilling rate reaching approximately 12,000 wells by 2050—a drilling activity that is orders-of-magnitude smaller than historic petroleum drilling activities. Development of CCS hubs focused around major industrial clusters and exploiting the storage resources available in the world's sedimentary basins offers an efficient and low-cost route to globally significant reductions in greenhouse gas emissions.

Although the most important challenges for future scale-up of CO_2 storage are socioeconomic, several technology developments could prove vital in reducing deployment costs and for stimulating widespread adoption of this climate mitigation tool. Key technology focus areas for the coming decade include

- further efforts to understand long-term stability and safety of CO_2 storage, by better understanding of fluid migration behavior, the rate of progress toward plume stability, and the rate of dissolution in the brine phase;
- development of smart and interactive ways of handling injectivity variations and formation pressure limits to enable optimal use of multiple storage units within sedimentary basins;
- further efforts on developing cost-effective monitoring solutions for assuring storage site performance, identifying anomalies, and modifying injection operations if needed (including fiber-optic solutions, trigger-survey concepts, and smart analysis of continuous and repeat-survey data sets); and
- development of CCS hubs with associated infrastructure (e.g., pipelines, wells, compressors, and control systems) to connect CO_2 capture points from major industrial clusters to multi-well storage systems in high-porosity sedimentary basins.

DISCLOSURE STATEMENT

ACKNOWLEDGMENTS

LITERATURE CITED

1. Metz B, ed. 2005. *Carbon Dioxide Capture and Storage: Special Report of the Intergovernmental Panel on Climate Change*. Cambridge, UK: Cambridge Univ. Press
2. Eide LI, Batum M, Dixon T, Elamin Z, Graue A, et al. 2019. Enabling large-scale carbon capture, utilisation, and storage (CCUS) using offshore carbon dioxide (CO_2) infrastructure developments—a review. *Energies* 12(10):1945
3. Harrison B, Falcone G. 2014. Carbon capture and sequestration versus carbon capture utilisation and storage for enhanced oil recovery. *Acta Geotech*. 9:29–38
4. Rani S, Padmanabhan E, Prusty BK. 2019. Review of gas adsorption in shales for enhanced methane recovery and CO_2 storage. *J. Pet. Sci. Eng.* 175:634–43
5. Godec M, Koperna G, Petrusak R, Oudinot A. 2014. Enhanced gas recovery and CO_2 storage in gas shales: a summary review of its status and potential. *Energy Procedia* 63:5849–57
6. Jenkins CR, Cook PJ, Ennis-King J, Undershultz J, Boreham C, et al. 2012. Safe storage and effective monitoring of CO_2 in depleted gas fields. *PNAS* 109(2):E35–E41
7. Godec M, Kuuskraa V, Van Leeuwen T, Melzer TL, Wildgust N. 2011. CO_2 storage in depleted oil fields: the worldwide potential for carbon dioxide enhanced oil recovery. *Energy Procedia* 4:2162–69

8. Busch A, Krooss BM, Gensterblum Y, Van Bergen F, Pagnier HJM. 2003. High-pressure adsorption of methane, carbon dioxide and their mixtures on coals with a special focus on the preferential sorption behaviour. *J. Geochem. Explor.* 78:671–74

9. Gislason SR, Oelkers EH. 2014. Carbon storage in basalt. *Science* 344(6182):373–74

10. Bentham M, Kirby M. 2005. CO_2 storage in saline aquifers. *Oil Gas Sci. Technol.* 60(3):559–67

11. Eiken O, Ringrose P, Hermanrud C, Nazarian B, Torp TA, Høier L. 2011. Lessons learned from 14 years of CCS operations: Sleipner, In Salah and Snøhvit. *Energy Procedia* 4:5541–48

12. Ringrose PS. 2018. The CCS hub in Norway: some insights from 22 years of saline aquifer storage. *Energy Procedia* 146:166–72

13. Ringrose PS, Meckel TA. 2019. Maturing global CO_2 storage resources on offshore continental margins to achieve 2DS emissions reductions. *Sci. Rep.* 9:17944

14. Int. Energy Agency. 2015. *Carbon Capture and Storage: The Solution for Deep Emissions Reductions*. Paris: Int. Energy Agency Publ.

15. Fuss S, Canadell JG, Peters GP, Tavoni M, Andrew RM, et al. 2014. Betting on negative emissions. *Nat. Climate Change* 4(10):850–53

16. Edenhofer O, Pichs-Madruga R, Sokona Y, Minx JC, Farahani E, et al., eds. 2014. *Mitigation of Climate Change: Working Group III Contribution to the Fifth Assessment Report of the Intergovernmental Panel on Climate Change*. Cambridge, UK: Cambridge Univ. Press

17. Masson-Delmotte V, ed. 2018. *Global warming of 1.5°C*. Spec. Rep., Intergov. Panel Clim. Change, Geneva, Switz.

18. Baklid A, Korbol R, Owren G. 1996. *Sleipner vest CO_2 disposal, CO_2 injection into a shallow underground aquifer*. Paper presented at the SPE Annual Technical Conference and Exhibition, Denver, CO, Oct.

19. Ampomah W, Balch R, Cather M, Rose-Coss D, Dai Z, et al. 2016. Evaluation of CO_2 storage mechanisms in CO_2 enhanced oil recovery sites: application to Morrow sandstone reservoir. *Energy Fuels* 30(10):8545–55

20. Pearce JM, Holloway S, Wacker H, Nelis MK, Rochelle C, Bateman K. 1996. Natural occurrences as analogues for the geological disposal of carbon dioxide. *Energy Conv. Manag.* 37(6–8):1123–28

21. Sathaye KJ, Hesse MA, Cassidy M, Stockli DF. 2014. Constraints on the magnitude and rate of CO_2 dissolution at Bravo Dome natural gas field. *PNAS* 111(43):15332–37

22. Gilfillan SM, Ballentine CJ, Holland G, Blagburn D, Lollar BS, et al. 2008. The noble gas geochemistry of natural CO_2 gas reservoirs from the Colorado Plateau and Rocky Mountain provinces, USA. *Geochim. Cosmochim. Acta* 72(4):1174–98

23. Burnside NM, Shipton ZK, Dockrill B, Ellam RM. 2013. Man-made versus natural CO_2 leakage: a 400 ky history of an analogue for engineered geological storage of CO_2. *Geology* 41(4):471–74

24. Nordbotten JM, Celia MA. 2012. *Geological Storage of CO_2: Modeling Approaches for Large-Scale Simulation*. Hoboken, NJ: John Wiley & Sons

25. Niemi A, Bear J, Bensabat J. 2017. *Geological Storage of CO_2 in Deep Saline Formations*. Dordrecht: Springer Neth.

26. Ringrose P. 2020. *How to Store CO_2 Underground: Insights from Early-Mover CCS Projects*. Cham, Switz.: Springer

27. Shook M, Li D, Lake LW. 1992. Scaling immiscible flow through permeable media by inspectional analysis. *In Situ* 16:4

28. Ringrose PS, Sorbie KS, Corbett PWM, Jensen JL. 1993. Immiscible flow behaviour in laminated and cross-bedded sandstones. *J. Pet. Sci. Eng.* 9(2):103–24

29. Zhou D, Fayers FJ, Orr FM Jr. 1997. Scaling of multiphase flow in simple heterogeneous porous media. *SPE Reserv. Eng.* 12(3):173–78

30. Oldenburg CM, Mukhopadhyay S, Cihan A. 2016. On the use of Darcy's law and invasion-percolation approaches for modeling large-scale geologic carbon sequestration. *Greenh. Gases* 6(1):19–33

31. Krevor SC, Pini R, Li B, Benson SM. 2011. Capillary heterogeneity trapping of CO_2 in a sandstone rock at reservoir conditions. *Geophys. Res. Lett.* 38(15). **https://doi.org/10.1029/2011GL048239**

32. Jackson SJ, Krevor S. 2020. Small-scale capillary heterogeneity linked to rapid plume migration during CO_2 storage. *Geophys. Res. Lett.* 47(18):e2020GL088616

33. Reynolds CA, Krevor S. 2015. Characterizing flow behavior for gas injection: relative permeability of CO-brine and N_2-water in heterogeneous rocks. *Water Resourc. Res.* 51(12):9464–89

34. Trevisan L, Pini R, Cihan A, Birkholzer JT, Zhou Q, Illangasekare TH. 2015. Experimental analysis of spatial correlation effects on capillary trapping of supercritical CO_2 at the intermediate laboratory scale in heterogeneous porous media. *Water Resourc. Res.* 51(11):8791–805

35. Krevor S, Blunt MJ, Benson SM, Pentland CH, Reynolds C, et al. 2015. Capillary trapping for geologic carbon dioxide storage—from pore scale physics to field scale implications. *Int. J. Greenh. Gas Control* 40:221–37

36. Meckel TA, Bryant SL, Ganesh PR. 2015. Characterization and prediction of CO_2 saturation resulting from modeling buoyant fluid migration in 2D heterogeneous geologic fabrics. *Int. J. Greenh. Gas Control* 34:85–96

37. Benham GP, Bickle MJ, Neufeld JA. 2020. Upscaling multiphase flow through heterogeneous porous media. arXiv. 2007.01540 [phys.flu-dyn]

38. Riaz A, Hesse M, Tchelepi HA, Orr FM. 2006. Onset of convection in a gravitationally unstable diffusive boundary layer in porous media. *J. Fluid Mech.* 548:87–111

39. Soltanian MR, Amooie MA, Gershenzon N, Dai Z, Ritzi R, et al. 2017. Dissolution trapping of carbon dioxide in heterogeneous aquifers. *Environ. Sci. Technol.* 51(13):7732–41

40. Gilmore KA, Neufeld JA, Bickle MJ. 2020. CO_2 dissolution trapping rates in heterogeneous porous media. *Geophys. Res. Lett.* 47(12):e2020GL087001

41. Alnes H, Eiken O, Nooner S, Sasagawa G, Stenvold T, Zumberge M. 2011. Results from Sleipner gravity monitoring: updated density and temperature distribution of the CO_2 plume. *Energy Procedia* 4:5504–11

42. Cavanagh AJ, Haszeldine RS, Nazarian B. 2015. The Sleipner CO_2 storage site: using a basin model to understand reservoir simulations of plume dynamics. *First Break* 33(6):61–68

43. Spycher N, Pruess K. 2009. A phase-partitioning model for CO_2-brine mixtures at elevated temperatures and pressures: application to CO_2-enhanced geothermal systems. *Transport Porous Media* 82:173–96

44. Amarasinghe W, Fjelde I, Rydland JA, Guo Y. 2019. *Effects of permeability and wettability on CO_2 dissolution and convection at realistic saline reservoir conditions: a visualization study*. Paper presented at the SPE Europec featured at 81st EAGE Conference and Exhibition, London, June

45. Gilfillan SM, Lollar BS, Holland G, Blagburn D, Stevens S, et al. 2009. Solubility trapping in formation water as dominant CO_2 sink in natural gas fields. *Nature* 458(7238):614–18

46. Zhou Z, Ballentine CJ, Schoell M, Stevens SH. 2012. Identifying and quantifying natural CO_2 sequestration processes over geological timescales: the Jackson Dome CO_2 Deposit, USA. *Geochim. Cosmochim. Acta* 86:257–75

47. Lollar BS, Ballentine CJ. 2009. Insights into deep carbon derived from noble gases. *Nat. Geosci.* 2(8):543–47

48. Györe D, Gilfillan SM, Stuart FM. 2017. Tracking the interaction between injected CO_2 and reservoir fluids using noble gas isotopes in an analogue of large-scale carbon capture and storage. *Appl. Geochem.* 78:116–28

49. Zwahlen CA, Kampman N, Dennis P, Zhou Z, Holland G. 2017. Estimating carbon dioxide residence time scales through noble gas and stable isotope diffusion profiles. *Geology* 45(11):995–98

50. Flude S, Johnson G, Gilfillan SM, Haszeldine RS. 2016. Inherent tracers for carbon capture and storage in sedimentary formations: composition and applications. *Environ. Sci. Technol.* 50(15):7939–55

51. Flude S, Györe D, Stuart FM, Zurakowska M, Boyce AJ, et al. 2017. The inherent tracer fingerprint of captured CO_2. *Int. J. Greenh. Gas Control* 65:40–54

52. Baines SJ, Worden RH. 2004. The long-term fate of CO_2 in the subsurface: natural analogues for CO_2 storage. *Geol. Soc.* 233:59–85

53. Land LS, Milliken KL, McBride EF. 1987. Diagenetic evolution of Cenozoic sandstones, Gulf of Mexico sedimentary basin. *Sediment. Geol.* 50(1–3):195–225

54. Carroll S, Carey JW, Dzombak D, Huerta NJ, Li L, et al. 2016. Role of chemistry, mechanics, and transport on well integrity in CO_2 storage environments. *Int. J. Greenh. Gas Control* 49:149–60

55. Black JR, Carroll SA, Haese RR. 2015. Rates of mineral dissolution under CO_2 storage conditions. *Chem. Geol.* 399:134–44

56. Wilkinson M, Haszeldine RS, Fallick AE, Odling N, Stoker SJ, Gatliff RW. 2009. CO_2–mineral reaction in a natural analogue for CO_2 storage—implications for modeling. *J. Sediment. Res.* 79(7):486–94

57. Busch A, Alles S, Gensterblum Y, Prinz D, Dewhurst DN, et al. 2008. Carbon dioxide storage potential of shales. *Int. J. Greenh. Gas Control* 2(3):297–308

58. Audigane P, Gaus I, Czernichowski-Lauriol I, Pruess K, Xu T. 2007. Two-dimensional reactive transport modeling of CO_2 injection in a saline aquifer at the Sleipner site, North Sea. *Am. J. Sci.* 307(7):974–1008

59. Carroll SA, McNab WW, Torres SC. 2011. Experimental study of cement-sandstone/shale-brine-CO_2 interactions. *Geochem. Trans.* 12:9

60. McNab WW, Carroll SA. 2011. Wellbore integrity at the Krechba Carbon Storage Site, In Salah, Algeria: 2. Reactive transport modeling of geochemical interactions near the cement–formation interface. *Energy Procedia* 4:5195–202

61. Aradóttir ES, Sigurdardóttir H, Sigfússon B, Gunnlaugsson E. 2011. CarbFix: a CCS pilot project imitating and accelerating natural CO_2 sequestration. *Greenh. Gases* 1(2):105–18

62. Watson MN, Boreham CJ, Tingate PR. 2004. Carbon dioxide and carbonate cements in the Otway Basin: implications for geological storage of carbon dioxide. *APPEA J.* 44(1):703–20

63. Li H, Yan J. 2009. Impacts of equations of state (EOS) and impurities on the volume calculation of CO_2 mixtures in the applications of CO_2 capture and storage (CCS) processes. *Appl. Energy* 86(12):2760–70

64. Span R, Gernert J, Jäger A. 2013. Accurate thermodynamic-property models for CO_2-rich mixtures. *Energy Procedia* 37:2914–22

65. Van der Meer LGH, Kreft E, Geel C, Hartman J. 2005. *K12-B a test site for CO_2 storage and enhanced gas recovery.* Paper presented at the SPE Europec/EAGE Annual Conference, Madrid, Spain, June

66. Nazarian B, Thorsen R, Ringrose P. 2018. *Storing CO_2 in a reservoir under continuous-pressure depletion*; *a simulation study*. Presented at the 14th Greenhouse Gas Control Technologies Conference, Melbourne, Aust., Oct. 21–26

67. Ringrose P, Greenberg S, Whittaker S, Nazarian B, Oye V. 2017. Building confidence in CO_2 storage using reference datasets from demonstration projects. *Energy Procedia* 114:3547–57

68. Hansen O, Gilding D, Nazarian B, Osdal B, Ringrose P, et al. 2013. Snøhvit: the history of injecting and storing 1 Mt CO_2 in the fluvial Tubåen Fm. *Energy Procedia* 37:3565–73

69. Hansen H, Eiken O, Aasum TA. 2005. *Tracing the path of carbon dioxide from a gas-condensate reservoir, through an amine plant and back into a subsurface aquifer—Case study: the Sleipner area, Norwegian North Sea*. Paper presented at the SPE Offshore Europe Oil and Gas Exhibition and Conference, Aberdeen, UK, Sept.

70. Huerta NJ, Cantrell KJ, White SK, Brown CF. 2020. Hydraulic fracturing to enhance injectivity and storage capacity of CO_2 storage reservoirs: benefits and risks. *Int. J. Greenh. Gas Control* 100:103105

71. Bachu S, Bonijoly D, Bradshaw J, Burruss R, Holloway S, et al. 2007. CO_2 storage capacity estimation: methodology and gaps. *Int. J. Greenh. Gas Control* 1(4):430–43

72. Vangkilde-Pedersen T, Anthonsen KL, Smith N, Kirk K, van der Meer B, et al. 2009. Assessing European capacity for geological storage of carbon dioxide—the EU GeoCapacity project. *Energy Procedia* 1(1):2663–70

73. Wright R, Mourits F, Rodríguez LB, Serrano MD. 2013. The first North American carbon storage atlas. *Energy Procedia* 37:5280–89

74. Riis F, Halland E. 2014. CO_2 storage atlas of the Norwegian Continental Shelf: methods used to evaluate capacity and maturity of the CO_2 storage potential. *Energy Procedia* 63:5258–65

75. Frailey SM, Tucker O, Koperna GJ. 2017. The genesis of the CO_2 storage resources management system (SRMS). *Energy Procedia* 114:4262–69

76. Thibeau S, Seldon L, Masserano F, Canal Vila J, Ringrose P. 2018. *Revisiting the Utsira saline aquifer CO_2 storage resources using the SRMS Classification Framework*. Presented at the 14th Greenhouse Gas Control Technologies Conference, Melbourne, Aust., Oct. 21–26

77. Van der Meer LGH. 1995. The CO_2 storage efficiency of aquifers. *Energy Convers. Manag.* 36(6):513–18

78. Trevisan L, Krishnamurthy PG, Meckel TA. 2017. Impact of 3D capillary heterogeneity and bedform architecture at the sub-meter scale on CO_2 saturation for buoyant flow in clastic aquifers. *Int. J. Greenh. Gas Control* 56:237–49

79. Krishnamurthy PG, Meckel TA, DiCarlo D. 2019. Mimicking geologic depositional fabrics for multiphase flow experiments. *Water Resourc. Res.* 55:9623–38

80. Nazarian B, Held R, Høier L, Ringrose P. 2013. Reservoir management of CO_2 injection: pressure control and capacity enhancement. *Energy Procedia* 37:4533–43

81. Birkholzer JT, Cihan A, Zhou Q. 2012. Impact-driven pressure management via targeted brine extraction—conceptual studies of CO_2 storage in saline formations. *Int. J. Greenh. Gas Control* 7:168–80

82. Santibanez-Borda E, Govindan R, Elahi N, Korre A, Durucan S. 2019. Maximising the dynamic CO_2 storage capacity through the optimisation of CO_2 injection and brine production rates. *Int. J. Greenh. Gas Control* 80:76–95

83. Anderson ST, Jahediesfanjani H. 2020. Estimating the net costs of brine production and disposal to expand pressure-limited dynamic capacity for basin-scale CO_2 storage in a saline formation. *Int. J. Greenh. Gas Control* 102:103161

84. Okwen RT, Stewart MT, Cunningham JA. 2010. Analytical solution for estimating storage efficiency of geologic sequestration of CO_2. *Int. J. Greenh. Gas Control* 4(1):102–7

85. Chadwick A, Arts R, Bernstone C, May F, Thibeau S, Zweigel P. 2008. *Best Practice for the Storage of CO_2 in Saline Aquifers: Observations and Guidelines from the SACS and CO2STORE Projects*, Vol. 14. Nottingham, UK: Br. Geol. Surv.

86. Jenkins C, Chadwick A, Hovorka SD. 2015. The state of the art in monitoring and verification—ten years on. *Int. J. Greenh. Gas Control* 40:312–49

87. Davis TL, Landrø M, Wilson M, eds. 2019. *Geophysics and Geosequestration*. Cambridge, UK: Cambridge Univ. Press

88. Furre AK, Eiken O, Alnes H, Vevatne JN, Kiær AF. 2017. 20 years of monitoring CO_2-injection at Sleipner. *Energy Procedia* 114:3916–26

89. Ringrose PS, Mathieson AS, Wright IW, Selama F, Hansen O, et al. 2013. The In Salah CO_2 storage project: lessons learned and knowledge transfer. *Energy Procedia* 37:6226–36

90. Huang F, Bergmann P, Juhlin C, Ivandic M, Lüth S, et al. 2018. The first post-injection seismic monitor survey at the Ketzin pilot CO_2 storage site: results from time-lapse analysis. *Geophys. Prospect.* 66(1):62–84

91. Tanase D, Saito H, Sasaki T, Tanaka Y, Tanaka J. 2018. *Progress of CO_2 injection and monitoring of the Tomakomai CCS Demonstration Project*. Presented at the 14th Greenhouse Gas Control Technologies Conference, Melbourne, Aust., Oct. 21–26

92. Bourne S, Crouch S, Smith M. 2014. A risk-based framework for measurement, monitoring and verification of the Quest CCS Project, Alberta, Canada. *Int. J. Greenh. Gas Control* 26:109–26

93. White D, Harris K, Roach L, Roberts B, Worth K, et al. 2017. Monitoring results after 36 ktonnes of deep CO_2 injection at the Aquistore CO_2 storage site, Saskatchewan, Canada. *Energy Procedia* 114:4056–61

94. Gilfillan S, Haszedline S, Stuart F, Gyore D, Kilgallon R, Wilkinson M. 2014. The application of noble gases and carbon stable isotopes in tracing the fate, migration and storage of CO_2. *Energy Procedia* 63:4123–33

95. Roberts JJ, Gilfillan SM, Stalker L, Naylor M. 2017. Geochemical tracers for monitoring offshore CO_2 stores. *Int. J. Greenh. Gas Control* 65:218–34

96. Ghaderi A, Landrø M. 2009. Estimation of thickness and velocity changes of injected carbon dioxide layers from pre-stack time-lapse seismic data. *Geophysics* 74:O17–28

97. Furre AK, Kiær A, Eiken O. 2015. CO_2-induced seismic time shifts at Sleipner. *Interpretation* 3(3):SS23–35

98. White J, Williams G, Chadwick AR, Furre A-K, Kiær A. 2018. Sleipner: the ongoing challenge to determine the thickness of a thin CO_2 layer. *Int. J. Greenh. Gas Control* 69:81–95

99. Chadwick RA, Williams GA, Falcon-Suarez I. 2019. Forensic mapping of seismic velocity heterogeneity in a CO_2 layer at the Sleipner CO_2 storage operation, North Sea, using time-lapse seismics. *Int. J. Greenh. Gas Control* 90:102793

100. Williams GA, Chadwick RA, Vosper H. 2018. Some thoughts on Darcy-type flow simulation for modelling underground CO_2 storage, based on the Sleipner CO_2 storage operation. *Int. J. Greenh. Gas Control* 68:164–75

101. Bickle M, Chadwick A, Huppert HE, Hallworth M, Lyle S. 2007. Modelling carbon dioxide accumulation at Sleipner: implications for underground carbon storage. *Earth Planet. Sci. Lett.* 255(1–2):164–76

102. Cavanagh AJ, Haszeldine RS. 2014. The Sleipner storage site: capillary flow modeling of a layered CO_2 plume requires fractured shale barriers within the Utsira Formation. *Int. J. Greenh. Gas Control* 21:101–12

103. Zadeh HM, Landrø M. 2011. Monitoring a shallow subsurface gas flow by time-lapse refraction analysis. *Geophysics* 76:O35–O43

104. Raknes EB, Arntsen B, Weibull W. 2015. Three-dimensional elastic full waveform inversion using seismic data from the Sleipner area. *Geophys. J. Int.* 202(3):1877–94

105. Mispel J, Furre A, Sollid A, Maaø FA. 2019. *High frequency 3D FWI at Sleipner: a closer look at the CO_2 plume*. Presented at the 81st EAGE Conference and Exhibition 2019, London, June 3–6

106. Landrø M. 2001. Discrimination between pressure and fluid saturation changes from time-lapse seismic data. *Geophysics* 66:836–44

107. Grude S, Landrø M, Osdal B. 2013. Time-lapse pressure-saturation discrimination for CO_2 storage at the Snøhvit field. *Int. J. Greenh. Gas Control* 19:369–78

108. Landrø M, Zumberge M. 2017. Estimating saturation and density changes caused by CO_2 injection at Sleipner—using time-lapse seismic amplitude-variation-with-offset and time-lapse gravity. *Interpretation* 5(2):T243–57

109. Zumberge M, Alnes H, Eiken O, Sasagawa G, Stenvold T. 2008. Precision of seafloor gravity and pressure measurements for reservoir monitoring. *Geophysics* 73(6):WA133–41

110. Mateeva A, Lopez J, Potters H, Mestayer J, Cox B, et al. 2014. Distributed acoustic sensing for reservoir monitoring with vertical seismic profiling. *Geophys. Prospect.* 62(4):679–92

111. Ringrose P, Furre AK, Bakke R, Dehghan Niri R, Paasch B, et al. 2018. *Developing optimised and cost-effective solutions for monitoring CO_2 injection from subsea wells*. Presented at the 14th Greenhouse Gas Control Technologies Conference, Melbourne, Aust., Oct. 21–26

112. Glob. CCS Inst. 2018. *Global Status of CCS: 2018*. Melbourne, Aust.: Glob. CCS Inst. **https://indd. adobe.com/view/2dab1be7-edd0-447d-b020-06242ea2cf3b**

113. Zahasky C, Krevor S. 2020. Global geologic carbon storage requirements of climate change mitigation scenarios. *Energy Environ. Sci.* 13:1561–67

114. Bachmann TM. 2020. Considering environmental costs of greenhouse gas emissions for setting a CO_2 tax: a review. *Sci. Total Environ.* 720:137524

115. EIA. 2020. *The distribution of U.S. oil and natural gas wells by production rate*. Press Rel., Dec. **https://www. eia.gov/petroleum/wells/**

116. Rubin ES, Davison JE, Herzog HJ. 2015. The cost of CO_2 capture and storage. *Int. J. Greenh. Gas Control* 40:378–400

117. Wu L, Thorsen R, Ottesen S, Meneguolo R, Hartvedt K, et al. 2021. Significance of fault seal in assessing CO_2 storage capacity and containment risks—an example from the Horda Platform, northern North Sea. *Pet. Geosci.* **https://doi.org/10.1144/petgeo2020-102**

Contents

Errata

An online log of corrections to *Annual Review of Chemical and Biomolecular Engineering*
articles may be found at http://www.annualreviews.org/errata/chembioeng